



# Contribution of TRESK two-pore domain potassium channel to bone cancer-induced spontaneous pain and evoked cutaneous pain in rats

Jiang-Ping Liu<sup>1,2</sup>, Hong-Bo Jing<sup>1,2</sup>, Ke Xi<sup>1,2</sup>, Zi-Xian Zhang<sup>1,2</sup>,  
Zi-Run Jin<sup>1,2</sup>, Si-Qing Cai<sup>1,2</sup>, Yue Tian<sup>1,2</sup>, Jie Cai<sup>1,2</sup>, and  
Guo-Gang Xing<sup>1,2,3,4</sup> 

Molecular Pain  
Volume 17: 1–18  
© The Author(s) 2021  
Article reuse guidelines:  
sagepub.com/journals-permissions  
DOI: 10.1177/17448069211023230  
journals.sagepub.com/home/mpx  


## Abstract

Cancer-associated pain is debilitating. However, the mechanism underlying cancer-induced spontaneous pain and evoked pain remains unclear. Here, using behavioral tests with immunofluorescent staining, overexpression, and knockdown of TRESK methods, we found an extensive distribution of TRESK potassium channel on both CGRP<sup>+</sup> and IB4<sup>+</sup> nerve fibers in the hindpaw skin, on CGRP<sup>+</sup> nerve fibers in the tibial periosteum which lacks IB4<sup>+</sup> fibers innervation, and on CGRP<sup>+</sup> and IB4<sup>+</sup> dorsal root ganglion (DRG) neurons in rats. Moreover, we found a decreased expression of TRESK in the corresponding nerve fibers within the hindpaw skin, the tibial periosteum and the DRG neurons in bone cancer rats. Overexpression of TRESK in DRG neurons attenuated both cancer-induced spontaneous pain (partly reflect skeletal pain) and evoked pain (reflect cutaneous pain) in tumor-bearing rats, in which the relief of evoked pain is time delayed than spontaneous pain. In contrast, knockdown of TRESK in DRG neurons produced both spontaneous pain and evoked pain in naïve rats. These results suggested that the differential distribution and decreased expression of TRESK in the periosteum and skin, which is attributed to the lack of IB4<sup>+</sup> fibers innervation within the periosteum of the tibia, probably contribute to the behavioral divergence of cancer-induced spontaneous pain and evoked pain in bone cancer rats. Thus, the assessment of spontaneous pain and evoked pain should be accomplished simultaneously when evaluating the effect of some novel analgesics in animal models. Also, this study provides solid evidence for the role of peripheral TRESK in both cancer-induced spontaneous pain and evoked cutaneous pain.

## Keywords

TRESK, bone cancer pain, CGRP, IB4, DRG, cancer-induced skeletal pain, cancer-induced cutaneous pain

Date Received: 20 October 2020; Revised 4 May 2021; accepted: 19 May 2021

## Introduction

Bone metastases are common complications of cancer, and metastatic cancer-induced bone pain is one of the most common types of pain in cancer patients.<sup>1</sup> Owing to the direct skeletal destruction in cancer progression, cancer-induced skeletal pain is an accurate and common assessment of bone cancer pain and can be measured by several skeletal pain-related behaviors such as limb use, weight bearing, and day/night activity.<sup>2,3</sup> Unfortunately, these skeletal pain-related behaviors are time and labor intensive. Recent studies have suggested that in humans and animals with significant skeletal pain, changes in

<sup>1</sup>Department of Neurobiology, School of Basic Medical Sciences, Peking University Health Science Center, Beijing, China

<sup>2</sup>Neuroscience Research Institute, Peking University, Beijing, China

<sup>3</sup>The Second Affiliated Hospital of Xinxiang Medical University, Xinxiang, China

<sup>4</sup>Key Laboratory for Neuroscience, Ministry of Education of China & National Health Commission of China, Beijing, China

The first two authors contributed equally to this work.

### Corresponding Author:

Guo-Gang Xing, Neuroscience Research Institute, Peking University, Beijing 100191, China; Department of Neurobiology, School of Basic Medical Sciences, Peking University Health Science Center, Beijing 100191, China.

Email: ggxing@bjmu.edu.cn



skin hypersensitivity can be detected.<sup>4-6</sup> Therefore, measurement of cancer-induced cutaneous pain, manifested as mechanical allodynia and thermal hyperalgesia, is proposed as a surrogate for assessing skeletal pain.<sup>7-10</sup> However, as the repertoire of sensory nerve fibers that innervate the skeleton is quite different from the repertoire of sensory nerve fibers that innervate the skin, thus the skeletal pain cannot be replaced by cutaneous pain simply and there seems to be a mechanistic decoupling between them. Using a battery of skeletal pain-related behaviors (e.g. spontaneous foot lifting, SFL, reduced weight-bearing, sporadic hopping, et al.) and von Frey assessment of mechanical hypersensitivity on the plantar surface of the hind paw (i.e. evoked pain), Guedon et al.<sup>11</sup> have identified the dissociation between the relief of skeletal pain behaviors and skin hypersensitivity in a mouse model of bone cancer pain. They demonstrated that anti-P2X3 showed a reduction in skin hypersensitivity but no attenuation of skeletal pain behaviors, whereas anti-nerve growth factor (NGF) showed a reduction in both skin hypersensitivity and skeletal pain behaviors. These results suggested that the relief of skin hypersensitivity may not always be a predictive surrogate for measuring the relief of underlying skeletal pain itself. Thus, understanding the relationship between skeletal and skin pain may provide insight into how pain is processed and integrated and help define the preclinical measures of skeletal pain that are predictive end points for clinical trials.

Accumulative evidence has documented that the differential distribution of peptide-rich calcitonin gene-related peptide (CGRP)- and peptide-poor isolectin B4 (IB4)-positive nerve fibers innervating the bone and skin, for instance, an abundant innervation of both CGRP<sup>+</sup> and IB4<sup>+</sup> nerve fibers within the skin, and a lack of IB4<sup>+</sup> nerve fibers innervation within the bone and joint, may underlie the dissociation between the cancer-induced skeletal pain and cutaneous pain.<sup>12-14</sup> CGRP<sup>+</sup> fibers have been shown to express substance P (SP) and tropomyosin receptor kinase A (TrkA), and be regulated by the corresponding ligand, nerve growth factor (NGF),<sup>15</sup> while IB4<sup>+</sup> fibers have been shown to express the purinergic P2X3 receptor and the GDNF receptor complex, and be regulated by glial cell line-derived neurotrophic factor (GDNF).<sup>16,17</sup> Thus, the purinergic P2X3 receptor is specifically required for the pathogenesis of cutaneous pain rather than skeletal pain, whereas NGF is required for the development of both pain phenotypes.<sup>11,18,19</sup>

In addition, sensitization of primary sensory neurons in dorsal root ganglion (DRGs) is critical for the development of bone cancer pain.<sup>20,21</sup> Abnormal changes of various ion channels in DRG neurons contribute to the hyperexcitability of nociceptive sensory neurons under pathological conditions,<sup>5,22-24</sup> among them, TWIK-related spinal cord K<sup>+</sup> channel (TRESK), a type of

two-pore-domain potassium channel (K<sub>2P</sub>), mediates major background currents in primary afferent neurons,<sup>25</sup> and plays an important role in the regulation of neuronal excitability.<sup>6,26-28</sup> In human and rodent tissue, TRESK is highly enriched in sensory ganglia of the DRG and trigeminal ganglion (TG).<sup>6,26,29</sup> Several RNA sequencing studies in DRG and TG ganglia have provided evidence showing that TRESK is present in a subpopulation of low-threshold mechanoreceptors involved in touch sensation (expressing TRKB and Piezo2) and, predominantly, in non-peptidergic nociceptors.<sup>30-32</sup> Using RNA *in situ* hybridization (ISH) and immunohistochemistry to define TRESK expression in the TG, Weir et al.<sup>33</sup> found TRESK expression to be highly heterogeneous across neurons. While expression data is somewhat conflicted,<sup>26,30,34</sup> it is consistently reported that TRESK is a K<sub>2P</sub> channel with a prominent role in pain pathways, and that loss of channel activity results in enhanced sensory neuron excitability and increased activation of *in vivo* pain pathways.<sup>26,27,34</sup> Guo et al.<sup>35</sup> found that endogenous TRESK activity regulates trigeminal nociception, and genetic loss of TRESK significantly increases the likelihood of developing headache. Royal et al.<sup>36</sup> demonstrated that migraine-associated frameshift mutations of TRESK lead to the production of a second protein fragment, which carries the pathophysiological function by inhibiting TREK1 and 2, due to a mechanism called frameshift mutation-induced alternative translation initiation (fsATI). Moreover, Castellanos et al.<sup>37</sup> discovered that genetic removal of TRESK specifically enhances mechanical and cold sensitivity in mice, not affecting the sensitivity to other stimuli. In rodent models of inflammatory pain, TRESK expression and TRESK-mediated background currents are decreased in the DRG, which contribute to the enhanced excitability of nociceptive sensory neurons.<sup>38,39</sup> TRESK gene (*Kcnk18*) silencing by RNA interference increases animals' sensitivity to painful stimuli,<sup>27</sup> whereas TRESK overexpression in DRG neurons reduces nerve trauma-induced mechanical allodynia in rats.<sup>40</sup> Both of the skeletal pain and cutaneous pain behaviors have been applied to assess the contribution of TRESK in pain signaling,<sup>38,40</sup> however, the underlying mechanisms of TRESK channels involved in the cancer-induced skeletal pain and cutaneous pain remain largely unclear.

In the present study, we investigated the role of TRESK in cancer-induced spontaneous pain (partly reflect skeletal pain) and evoked pain (reflect cutaneous pain) in tumor-bearing rats. We found that the differential distribution and the decreased expression of TRESK channels in the periosteum and skin, which is attributed to the lack of IB4<sup>+</sup> fibers innervation within the periosteum of the tibia, probably contribute to the behavioral

divergence of cancer-induced spontaneous pain and evoked pain in bone cancer rats.

## Materials and methods

### Animals

Adult female Sprague-Dawley rats weighing 150–200g at the beginning of the experiment were provided by the Department of Experimental Animal Sciences, Peking University Health Science Center. The rats were housed in separated cages with free access to food and water. The room temperature was kept at  $25 \pm 1^\circ\text{C}$  under a 12-h light–dark cycle. All animal experimental procedures were carried out in accordance with the guidelines of the International Association for the Study of Pain<sup>41</sup> and were approved by the Animal Care and Use Committee of Peking University. The behavioral experimenters were kept blind from the groupings of the rats.

### Animal model of bone cancer pain

A rat model of bone cancer pain was established by intratibial injections of syngeneic rat breast carcinoma cells (MRMT-1) as previously described.<sup>5,6,42</sup> Briefly, after anesthetized with pentobarbital sodium (50 mg/kg, intraperitoneal injection, i.p.), the left tibia of rat was carefully exposed and a 23-gauge needle was inserted in the intramedullary canal of the bone. It was then removed and replaced with a long, thin blunt needle attached to a 10- $\mu\text{l}$  Hamilton syringe containing the medium to be injected. A volume of 4  $\mu\text{l}$  of MRMT-1 tumor cells ( $4 \times 10^4$ ) or vehicle (PBS) was injected into the tibial bone cavity. After injection, the site was sealed with bone wax, and the wound was finally closed. Any rats exhibiting motor deficiency or lack of pain hypersensitivity after tumor cell inoculation, as well as those that died during the experiments, were excluded from the study.

### Behavioral studies

Rats were acclimatized to the testing environment for 30 minutes on 4 consecutive days 1 week before naive baseline behavioral testing. All behavioral testing was performed in the morning and completed before noon. Testing was performed at baseline (pre-sarcoma inoculation) and 7, 14, and 18 days post-sarcoma inoculation. As described in previous studies,<sup>12–14</sup> spontaneous nociceptive behavioral indicators of pain, that is, spontaneous foot-lifting (SFL) behaviors including SFL duration (SFLd) and numbers (SFLn) were assessed for skeletal pain, while cutaneous stimulus-evoked pain such as mechanical withdrawal thresholds to von Frey filaments stimuli and paw withdrawal latency to radiant heat

stimulation were assessed for cutaneous pain. Each individual behavioral measure was performed by the same experimenter for the duration of the experiment. These individuals were blinded to the treatments of animals received.

**Assessment of spontaneous pain.** As described in previous reports,<sup>6,43</sup> spontaneous foot-lifting (SFL) behavior including SFL duration (SFLd) and number (SFLn) is a useful assessment for spontaneous pain. In brief, rats were placed in a clear plastic box with a glass floor. SFL was not measured until the rats had finished exploring and grooming. The SFLd was the cumulative amount of time that the left hindpaw was lifted over 10 minutes (two 5-min periods separated by an interval over 5 minutes). Lifts or flicks of the foot/leg which were too short to measure accurately were recorded as 0.5 seconds. The SFLn was recorded simultaneously during the same duration. Foot lifting associated with exploratory behavior, locomotion and grooming was excluded from the test.

**Assessment of mechanical allodynia.** Mechanical allodynia was assessed by measuring 50% paw withdrawal threshold (PWT) as described in our previous studies.<sup>5,44</sup> The PWT in response to a series of von Frey filament (Stoelting, Wood Dale, US) was determined by the up-down method.<sup>45</sup> Briefly, the rat was placed on a metal mesh floor covered with a clear plastic cage ( $18 \times 8 \times 8\text{cm}$ ) and allowed a habituation period for 20 minutes. Eight von Frey filaments with approximately equal logarithmic incremental bending forces (0.224) were chosen (0.41, 0.70, 1.20, 2.00, 3.63, 5.50, 8.50, and 15.10g). Each test started with a 2.00g von Frey filament which was delivered perpendicularly to the plantar surface of the left hindpaw for 2 to 3 seconds. Abrupt withdrawal of the foot during stimulation or immediately after the removal of the filament was regarded as a positive response. Whenever there was a positive or negative response, the next weaker or stronger filament was applied, respectively. This procedure was completed until 6 stimuli after the first change in response had been observed. The 50% PWT was calculated using the following formula: 50% PWT (g) =  $(10^{[X_f + \kappa\delta]})$ , where  $X_f$  is the value of the final von Frey filament used (in log units),  $\kappa$  is a value acquired from the pattern of positive/negative response, and  $\delta$  is the average interval (0.224, in log units) between the von Frey filaments.<sup>46</sup> An allodynia rat is defined as whose 50% PWT is less than 4.0g (i.e., withdrawal in response to non-noxious tactile stimulus).<sup>47</sup>

**Assessment of thermal hyperalgesia.** Thermal hyperalgesia of the hind paws was tested as described in our previous reports.<sup>5,44</sup> Rats were allowed to acclimate for at least 30

minutes within acrylic enclosures on a clear glass plate before testing. A radiant heat source was focused onto the plantar surface of the left hindpaw. Paw withdrawal latency (PWL) were measured by a timer that was started by the activation of the heat source and stopped when the withdrawal of the paw was detected. A maximal cut-off time of 30 seconds was used to prevent unnecessary tissue injury. Three measurements of PWL at 5-minute intervals were taken and averaged as the final result data.

### *Immunofluorescent staining*

Deeply anesthetized rats were perfused with 250 ml of normal saline followed by 200 ml of 4% paraformaldehyde (in 0.1 M phosphate buffer [PB], pH 7.4). The preparation of periosteum (representative of bone), glabrous skin, as well as DRG and the spinal cord tissues were performed as previously described.<sup>12</sup> Periosteums from the ipsilateral tibia diaphysis were removed for a whole mount. The periosteum was harvested from the distal growth plate region to immediately below the third trochanter by performing a vertical cut along the boundary of the desired area on the bone with a scalpel blade. Under a stereoscope, the periosteum was removed gently by scraping against the bone with forceps. The whole-mount preparations of periosteum were placed in PBS for further processing. The ipsilateral glabrous skin of hindpaws, the L4/5 DRGs and the spinal cord were quickly removed, post-fixed in the same fixative solution for 4 hours and then were cryoprotected in 30% sucrose (in 0.1M PB). Several days later, frozen glabrous skin of the hindpaw (40- $\mu$ m thick) sections and DRG (10- $\mu$ m thick) sections were cut on a cryostat and collected in PBS or mounted on adhesion microscope slides for the following staining. For immunofluorescent staining, tissues were blocked in 10% goat serum (in 0.1M PBS) with 0.3% Triton-X 100 for 1 hour at room temperature after being washed three times by PBS for 5 minutes each. Then, tissues were incubated with the respective primary antibody in PBS at 4°C overnight, which includes rabbit anti-TRESK (1:200, APC-122, Alomone Labs, Jerusalem, Israel), mouse anti-CGRP (1:200, Abcam, Cambridge, US), mouse anti-NeuN (1:200, MAB377, Merck Millipore, Billerica, MA, USA), mouse anti-NF200 (1:200, N0142, Sigma-Aldrich, St. Louis, MO, USA), mouse anti-UCHL1 (i.e. PGP9.5, 1:200, AMAB91145, Merk-Millipore), mouse anti-EpCAM (1:500, MA512436, Invitrogen), and rabbit anti-KCNK18 (TRESK) (1:200, APC-122, Alomone). Control sections (the negative control) were processed without the addition of primary antibody. After three washes in PBS, the tissues were incubated with the following secondary antibody at room temperature for 1 hour: tetramethylrhodamine

(TRITC)-labeled goat anti-rabbit IgG (1:200, ZSGB-BIO, Beijing, China), fluorescein isothiocyanate (FITC)-labeled goat anti-mouse IgG (1:200, ZSGB-BIO, Beijing, China), and Alexa Fluor 647 goat anti-mouse IgG (1:200, Bioss, Beijing, China). For IB4 staining, the tissues were incubated with IB4-FITC (10  $\mu$ g/ml, Sigma-Aldrich, Saint Louis, US) for 2 hours at 37°C. The fluorescence signal was detected by confocal microscopy at excitation wavelengths of 488nm (green), 543 nm (red) and 647 nm (blue). At least three fields per section were analyzed to avoid bias, and at least three independent experiments were performed for immunostaining.

### *Neutralizing peptide blocking experiment*

The specificity validation of anti-TRESK was carried out via a neutralizing peptide blocking experiment using a specific blocking peptide targeting anti-TRESK antibody. In brief, before proceeding with the immunoblot protocol, the antibody was neutralized by co-incubation with a specific blocking peptide that corresponds to the epitope recognized by the antibody. The antibody that was bound to the blocking peptide was no longer available to bind to the epitope present in the protein. The neutralized antibody was then used side by side with the antibody alone, and the results were compared. By comparing the immunoblot from the blocked antibody versus the antibody alone. The specific immunoblot signal was blocked by pre-incubation with a specific blocking peptide, but not by a control peptide IgG. The specificity of anti-TRESK antibody was determined by specific inhibition of TRESK immunoblot after co-incubation with a specific blocking peptide targeting the TRESK antibody.

### *Implantation of intrathecal catheter*

Under pentobarbital sodium (50 mg/kg, i.p.) anesthesia, implantation of intrathecal cannula was carried out as described in our previous study.<sup>44</sup> That is, a PE-10 polyethylene catheter was implanted between the L5 and L6 vertebrae to reach the lumbar enlargement of the spinal cord. The correct intrathecal localization was confirmed by a tail-flick or a paw retraction, by easy insertion of a catheter through the cannula, and occasionally by a backflow of spinal fluid. The outer part of the catheter was plugged and fixed onto the skin upon closure of the wound. All surgical procedures were completed in sterile conditions. Rats showing neurological deficits after the catheter implantation were excluded from the experiment.

### *Lentivirus infection and siRNA injection*

Construction and production of recombinant lentivirus expressing TRESK linked with ZsGreen (LV-TRESK)

were completed by BioWit Technologies (Shenzhen, China) using pLVX-mCMV-ZsGreen vector and the rTRESK-pcDNA3.1 plasmid (provided by X. Gasull in University of Barcelona, Barcelona, Spain). For the *in vivo* studies, lentivirus, including LV-TRESK and its control LV-ZsGreen, was intrathecally administered to rats at a final titer of  $4 \times 10^8$  transducing units/ml (in a 25- $\mu$ l volume of solution), respectively. The lentivirus was intrathecally delivered to animals on day 7 after sarcoma inoculation based on our previous findings. Overexpression efficiency was determined by RT-qPCR and Western blotting.

Targeted siRNAs were applied to knock down the abundance of TRESK. Briefly, three siRNAs targeting rat TRESK mRNA were designed and synthesized by Invitrogen Technologies (Carlsbad, US). Knockdown efficiency was determined by RT-qPCR and Western blotting. The preliminary experiments showed that intrathecal injection of TRESK siRNA3 (2 $\mu$ g in a 10- $\mu$ l volume) could significantly inhibit the abundance of TRESK protein in the DRG. Hence, the synthesized TRESK siRNA3 was chosen for the present study. TRESK siRNA was intrathecally administered to the naïve rats once per day and continued for 2 days. Sequences of the three TRESK siRNAs are listed as follows:

TRESK siRNA1 forward, 5'-GACAGUGGUUGA AGGUAGCAGGAAA-3', reverse, 5'-UUUCCUGCU ACCUUAACCACUGUC-3';

TRESK siRNA2 forward, 5'-CACAUCCUGGCCG CCAUCUUAUCUA-3', reverse, 5'-UAGAUAGAU GCGCGCCAGGAUGUC-3';

TRESK siRNA3 forward, 5'-GCACAGUGUUCAG CACAGUGGGUUA-3', reverse, 5'-UAACCCACUGU GCUGAACACUGUGC-3'.

### RNA extraction and RT-qPCR

Total RNA of the ipsilateral rat L4/5 DRG was extracted with TRIzol reagent (Life Technologies, Carlsbad, US) according to the operational instructions. Reverse transcription was performed with 1 $\mu$ g of total RNA by using PrimeScript RT-PCR kit (Takara Bio, Dalian, China) according to the manufacturer's instructions.

Real-time quantitative PCR (RT-qPCR) was performed on an ABI 7500 Real-Time PCR System (Applied Biosystems, Foster City, US) with GoTaq<sup>®</sup> qPCR Master Mix (Promega, Madison, US). Data was expressed as  $2^{-\Delta\Delta C_t}$ , that is, the fold change in TRESK mRNA. The following primers were used for RT-qPCR reactions: TRESK forward 5'-CTCACTTCTTCTTCTTCTTCTC-3', reverse 5'-TAGCAAGGTAGCGAA ACCTCT-3';  $\beta$ -actin forward 5'-AGCCATGTACG TAGCCATCC-3', reverse 5'-GCCATCTCTTGCTC GAAGTC-3'

### Western blot

Rats were deeply anesthetized with pentobarbital sodium (50 mg/kg, *i.p.*) and then the ipsilateral L4/5 DRG were removed and homogenized in cold lysis buffer containing 50mM Tris (pH 8.0), 150mM NaCl, 1% Nonidet P 40 (NP40), 0.5% sodium deoxycholate, 0.1% sodium dodecyl sulfate (SDS), and protease inhibitor cocktail (Roche, Indianapolis, US). The homogenates were centrifuged at 12,000g for 10 minutes at 4°C, and then the supernatant was analyzed. The concentration of protein was measured with a BCA assay kit (Pierce, Rockford, US), and the sample containing 60 $\mu$ g of protein were denatured and then separated through polyacrylamide gel electrophoresis (SDS-PAGE) using 10% separating gels and transferred to a polyvinylidene fluoride (PVDF) membrane (Bio-Rad, Hercules, US). After blocking with 5% nonfat milk in TBST (20mM Tris-HCl, pH 7.5, 150mM NaCl, and 0.05% Tween-20) for 1 hour at room temperature, the membranes were incubated with primary antibody, rabbit anti-TRESK (1:1000, Alomone, Jerusalem, Israel), or mouse anti- $\beta$ -actin (1:2000, Santa Cruz Biotechnology, Santa Cruz, US), at 4°C overnight. The blots were washed in TBST and then incubated in horseradish peroxidase (HRP)-conjugated secondary antibody (1:2000, goat anti-rabbit or mouse, Santa Cruz Biotechnology, Santa Cruz, US). Protein bands were visualized using an enhanced chemiluminescence detection kit (Pierce, Rockford, US) followed by photography using a chemiluminescent imaging system (Tanon Science & Technology, Shanghai, China). The standardized ratio of TRESK to  $\beta$ -actin band density was used to calculate the alteration in TRESK expression.

### Statistical analysis

Statistical analyses were performed with GraphPad Prism 8.0 for Window (GraphPad Software Inc., La Jolla, CA). All quantitative biochemical data and histological staining are representative of at least three independent experiments. Shapiro-Wilkes tests were used to assess normality in the distribution (Gaussian distribution) for each group, and only the data were normally distributed and variances were similar between groups to be compared were subjected to parametric statistical tests, otherwise specific nonparametric tests were applied as indicated in the text. Two-tailed unpaired Student's *t* test was used for the comparison of the mean values between two groups. One-way ANOVA with Tukey's *post-hoc* test, or two-way ANOVA (treatment and time factors) with Sidak's *post-hoc* test was used for multiple comparison. All data are expressed as means  $\pm$  SEM, and differences with  $p < 0.05$  were considered statistically significant. The significant differences between groups were represented as \* $p < 0.05$ , \*\* $p < 0.01$ , and \*\*\* $p < 0.001$ .

## Results

### *Distribution of TRESK in the nerve fibers innervating the tibial periosteum and the hindpaw skin in naïve rats*

It has been established that TRESK channel mediates major background currents in primary afferent neurons and determines neuronal excitability.<sup>25,27</sup> Although the existence of TRESK has been confirmed in DRG neurons, the expression of TRESK in primary afferent nerve fibers that innervate the bone and skin is still unknown. The main nerve fibers mediating nociception are peptide-rich CGRP<sup>+</sup>- and peptide-poor IB4<sup>+</sup>-C fibers. We first examined the distribution of TRESK channels in these types of sensory nerve fibers within the tibial periosteum and the hindpaw skin in naïve rats by immunofluorescence staining with TRESK and CGRP (or IB4). The specificity of TRESK antibody was verified by using immunocytochemistry and Western blot, including a neutralizing peptide-blocking experiment (i.e. with pre-absorbed antibody) with TRESK-transfected and non-transfected human embryonic kidney (HEK) 293 cells, which do not express endogenous TRESK (Supplementary material, Fig. S1). Consistent with previous findings,<sup>12,48,49</sup> we found a lack of IB4<sup>+</sup> fibers innervation within the periosteum of the tibia, while both CGRP<sup>+</sup> and IB4<sup>+</sup> nerve fibers were present in the glabrous skin of the hindpaw in rats (Figure 1(a)). Moreover, the results revealed that TRESK was widely expressed on these two types of nerve fibers (Figure 1(a) and (b)), and accordingly, a co-localization of TRESK with both CGRP<sup>+</sup> and IB4<sup>+</sup> nerve fibers were found in the glabrous skin of the hindpaw (Figure 1(b)), whereas in the periosteum, the TRESK was only expressed on the CGRP<sup>+</sup> nerve fibers due to the lack of IB4<sup>+</sup> fibers innervation (Figure 1(a)). Furthermore, a co-staining of TRESK with nerve fiber markers NF200 (the large fiber marker) and PGP9.5/UCHL1 (the small fiber marker), as well as with the epidermal cell marker, EpCAM has been performed in the glabrous skin of hindpaws in naïve rats. The results showed that the TRESK staining seems rather large in many parts of the skin including dermal and epidermal cells, even with the neuronal markers, NF200 (the large fiber marker, Figure 2(a)) and PGP9.5/UCHL1 (the small fiber marker, Figure 2(b)), as well as with the epidermal cell marker, EpCAM (Figure 2(c)). Together, these results suggested that although the TRESK was widely expressed on both CGRP<sup>+</sup> and IB4<sup>+</sup> nerve fibers, however, that the lack of IB4<sup>+</sup> fibers innervation within the periosteum of the tibia will result in the differential distribution of TRESK in the nerve fibers innervating the tibial periosteum and the hindpaw skin in rats.

### *Decreased expression of TRESK in the tibial periosteum, the hindpaw skin and the nociceptive DRG neurons in bone cancer rats*

Next, we investigated the alternation of TRESK expression in the corresponding nerve fibers innervating the tibial periosteum and the hindpaw skin in rats with bone cancer pain. A reduction of TRESK expression on these fibers was found in the ipsilateral tibial periosteum and hindpaw skin of tumor-bearing (MRMT-1) rats (Figure 3). The mean fluorescence intensity of co-expressed TRESK with CGRP<sup>+</sup> fibers was significantly decreased in ipsilateral tibial periosteum in tumor-bearing rats ( $21.1 \pm 2.4$ ) compared with controls of naïve ( $58.3 \pm 2.4$ ) and PBS ( $56.5 \pm 2.3$ )-treated rats on day 14 post-surgery ( $p < 0.0001$ ,  $F_{2,24} = 76.29$ , one-way ANOVA, Figure 3(a) and (b)). Likewise, the mean fluorescence intensity of co-expressed TRESK with both CGRP<sup>+</sup> fibers (MRMT-1  $35.5 \pm 2.4$  vs. naïve  $54.6 \pm 4.3$ ,  $p = 0.0015$ ; vs. PBS  $53.1 \pm 3.2$ ,  $p = 0.0034$ ,  $F_{2,24} = 9.82$ , one-way ANOVA, Figure 3(c) and (d)) and IB4<sup>+</sup> fibers (MRMT-1  $38.2 \pm 3.1$  vs. naïve  $57.4 \pm 3.8$ ,  $p = 0.0015$ ; vs. PBS  $56.8 \pm 3.3$ ,  $p = 0.0021$ ,  $F_{2,24} = 10.25$ , one-way ANOVA, Figure 3(e) and (f)) was also decreased in the glabrous skin of the hindpaw in tumor-bearing rats compared with naïve and PBS rats on day 14 post-surgery.

Furthermore, we examined the TRESK expression on their corresponding cell bodies in DRG neurons. We found a wide expression of TRESK on both peptide-rich CGRP<sup>+</sup> (Figure 4(a)) and peptide-poor IB4<sup>+</sup> DRG neurons (Figure 4(c)). Also, a significant decrease of TRESK immunofluorescence intensity in CGRP<sup>+</sup> neurons (MRMT-1  $21.6 \pm 0.6$  vs. naïve  $73.1 \pm 1.4$ , vs. PBS  $70.6 \pm 1.6$ ,  $p < 0.0001$ ,  $F_{2,317} = 552.1$ , one-way ANOVA, Figure 4(b)) and IB4<sup>+</sup> neurons (MRMT-1  $34.8 \pm 0.9$  vs. naïve  $60.5 \pm 1.3$ , vs. PBS  $64.7 \pm 1.4$ ,  $p < 0.0001$ ,  $F_{2,294} = 178.6$ , one-way ANOVA, Figure 4(d)) was observed in ipsilateral L4/5 DRG neurons in tumor-bearing rats on day 14 post-surgery. Moreover, using real-time quantitative PCR (RT-qPCR) and Western blotting, we also examined the alterations of TRESK abundance, at the protein and mRNA levels, in ipsilateral L4/5 DRGs from rats at 14 days after implantation of MRMT-1 tumor cells into the tibial bone cavity. We found a concomitant and significant decrease in TRESK mRNA (MRMT-1  $0.46 \pm 0.05$  vs. naïve  $1.08 \pm 0.10$ , vs. PBS  $1.05 \pm 0.09$ ,  $p = 0.0001$  compared between MRMT-1 and naïve,  $p = 0.0002$  compared between MRMT-1 and PBS,  $F_{2,18} = 17.80$ , one-way ANOVA, Figure 4(e)) and protein (MRMT-1  $0.43 \pm 0.07$  vs. PBS  $1.04 \pm 0.05$ ,  $p < 0.0001$ ,  $F_{2,42} = 14.63$ , two-way ANOVA, Figure 4(f)) abundance in ipsilateral L4/5 DRGs in tumor-bearing rats on day 14 post-surgery. These results suggested that the TRESK expression was reduced in DRG neurons innervating both the tibial periosteum

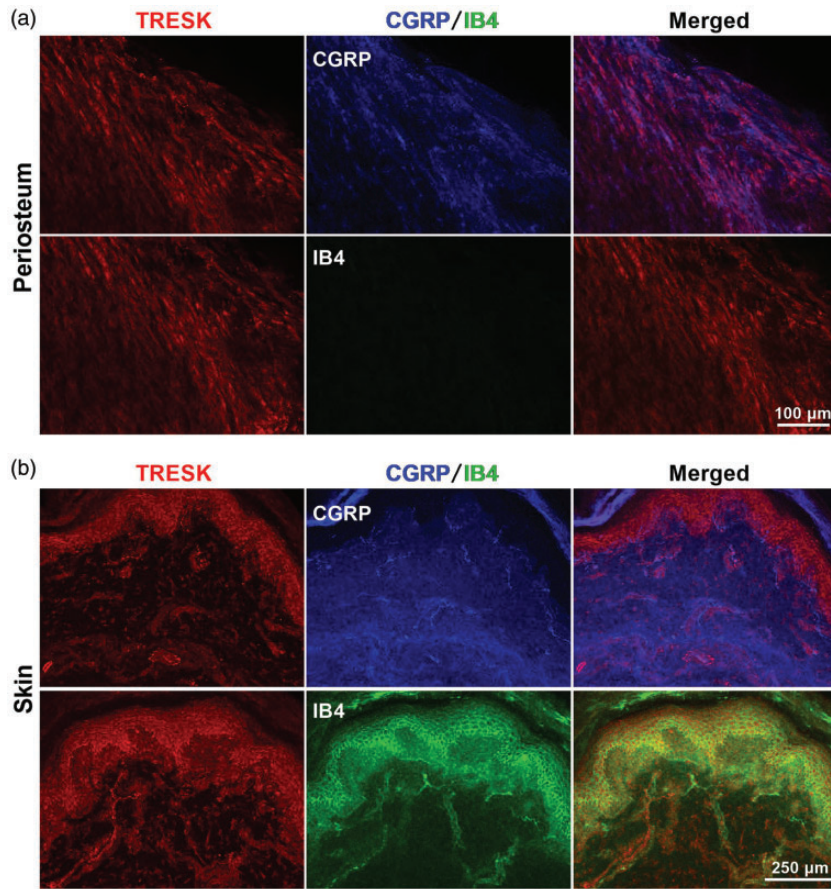


**Figure 1.** Distribution of TRESK in primary afferent nerve fibers innervating the tibial periosteum and the hindpaw skin in naïve rats. (a) Representative images of immunofluorescence staining with TRESK (red) and CGRP (blue)/IB4 (green) in the tibial periosteum are shown. Note that due to the lack of IB4<sup>+</sup> fibers innervation within the tibial periosteum, the TRESK is merely co-expressed with CGRP<sup>+</sup> nerve fibers in the tibial periosteum. Scale bar = 100 μm,  $n = 3$  independent experiments. (b) Shown are representative images of immunofluorescence staining with TRESK (red) and CGRP (blue)/IB4 (green) in the hindpaw skin. Note that a co-localization of TRESK with both CGRP<sup>+</sup> and IB4<sup>+</sup> nerve fibers is found in the hindpaw skin. Scale bar = 250 μm,  $n = 3$  independent experiments.

and the ipsilateral hindpaw skin in rats, where a decreased expression of TRESK was present in both CGRP<sup>+</sup> and IB4<sup>+</sup> nerve fibers within the hindpaw skin and DRG neurons, while in CGRP<sup>+</sup> nerve fibers within the tibial periosteum due to the lack of IB4<sup>+</sup> fibers innervation within the periosteum of the tibia.

#### ***Overexpression of TRESK in DRG neurons attenuates the spontaneous pain and evoked pain behaviors in bone cancer rats***

To elucidate whether the decreased expression of TRESK in tibial periosteum, hindpaw skin and DRG neurons contribute to the pathogenesis of bone cancer-induced spontaneous pain and evoked pain, we investigated the effects of TRESK overexpression on both spontaneous pain (spontaneous foot-lifting behaviors) and evoked cutaneous pain (mechanical allodynia, paw withdrawal threshold in response to von Frey filaments;

and thermal hyperalgesia, paw withdrawal latency in response to radiant heat) in bone cancer rats. Overexpression of TRESK protein in DRG neurons was validated by enhanced fluorescence intensity of TRESK in LV-TRESK infected DRG neurons using immunostaining with TRESK and lentivirus-linked ZsGreen (Figure 5(a)) and increased expression of TRESK protein using Western blotting assay (LV-TRESK  $1.2 \pm 0.1$  vs. LV-ZsGreen  $0.5 \pm 0.1$ ,  $p = 0.0015$ ,  $t_6 = 5.54$ , unpaired two-tailed t-test, Figure 5(b)) in DRG tissues obtained from tumor-bearing rats on day 7 after intrathecal injection (i.t.) of lentivirus-expressed TRESK linked ZsGreen (LV-TRESK). Also, intrathecal injection of LV-TRESK increases TRESK expression in the spinal cord neurons (Supplementary materials, Fig. S2). The behavioral results showed that overexpression of TRESK attenuated both the bone cancer-induced spontaneous pain and evoked pain in tumor-bearing rats, in which the reduction of evoked cutaneous pain

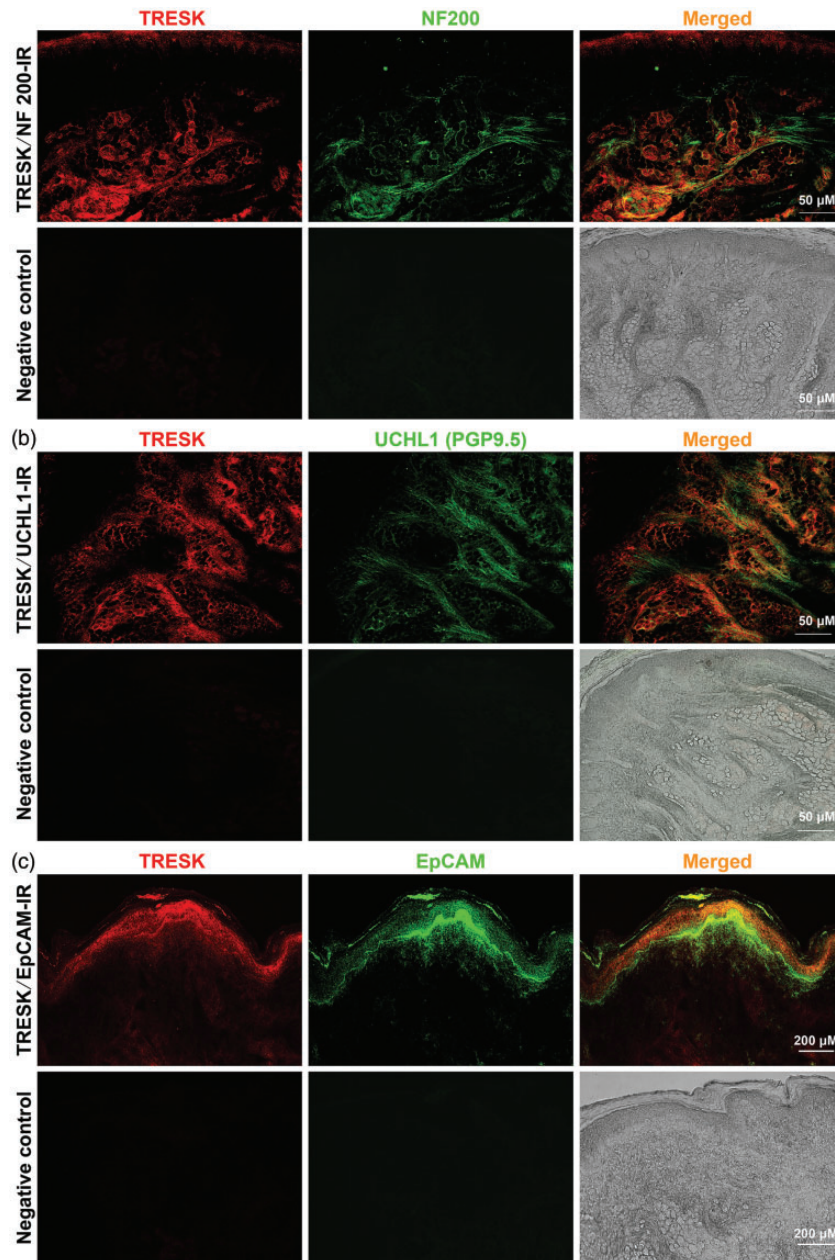


**Figure 2.** Double immunofluorescent staining of TRESK with NF200, UCHL1 (PGP9.5), and EpCAM in the hindpaw skin of rats. (a) Representative images of immunofluorescence staining with TRESK (red) and NF200 (the large nerve fiber marker, green) are shown (upper). Lower, negative controls omitting the primary antibody. (b) Representative images of immunofluorescence staining with TRESK (red) and UCHL1 (PGP9.5) (the small nerve fiber marker, green) are shown (upper). Lower, negative controls omitting the primary antibody. (c) Representative images of immunofluorescence staining with TRESK (red) and EpCAM (the epidermal cell marker, green) are shown (upper). Lower, negative controls omitting the primary antibody. Scale bar = 50  $\mu\text{m}$  for (a) and (b), Scale bar = 200  $\mu\text{m}$  for (c),  $n = 3$  independent experiments.

is delayed than evoked pain in the time course after LV-TRESK application (Figure 5(c) to (f)). In contrast, overexpression of TRESK by intrathecal injection of LV-TRESK did not affect the evoked pain behaviors in control (PBS) rats (Figure 5(e) and (f)). For example, the bone cancer-induced spontaneous pain, as indicated by spontaneous foot-lifting (SFL) behaviors including

SFL duration (SFLd) and numbers (SFLn), were relieved on day 14 after tumor cells inoculation (SFLd: LV-TRESK  $1.0 \pm 0.2$  sec vs. LV-ZsGreen  $2.9 \pm 0.6$  sec,  $p = 0.04$ ,  $F_{3,68} = 3.2$ ; SFLn: LV-TRESK  $2.8 \pm 0.6$  events vs. LV-ZsGreen  $6.9 \pm 1.2$  events,  $p = 0.0337$ ,  $F_{3,45} = 3.13$ , two-way ANOVA, Figure 5(c) and (d)) and lasted to day 18 after tumor cells inoculation (SFLd: LV-TRESK



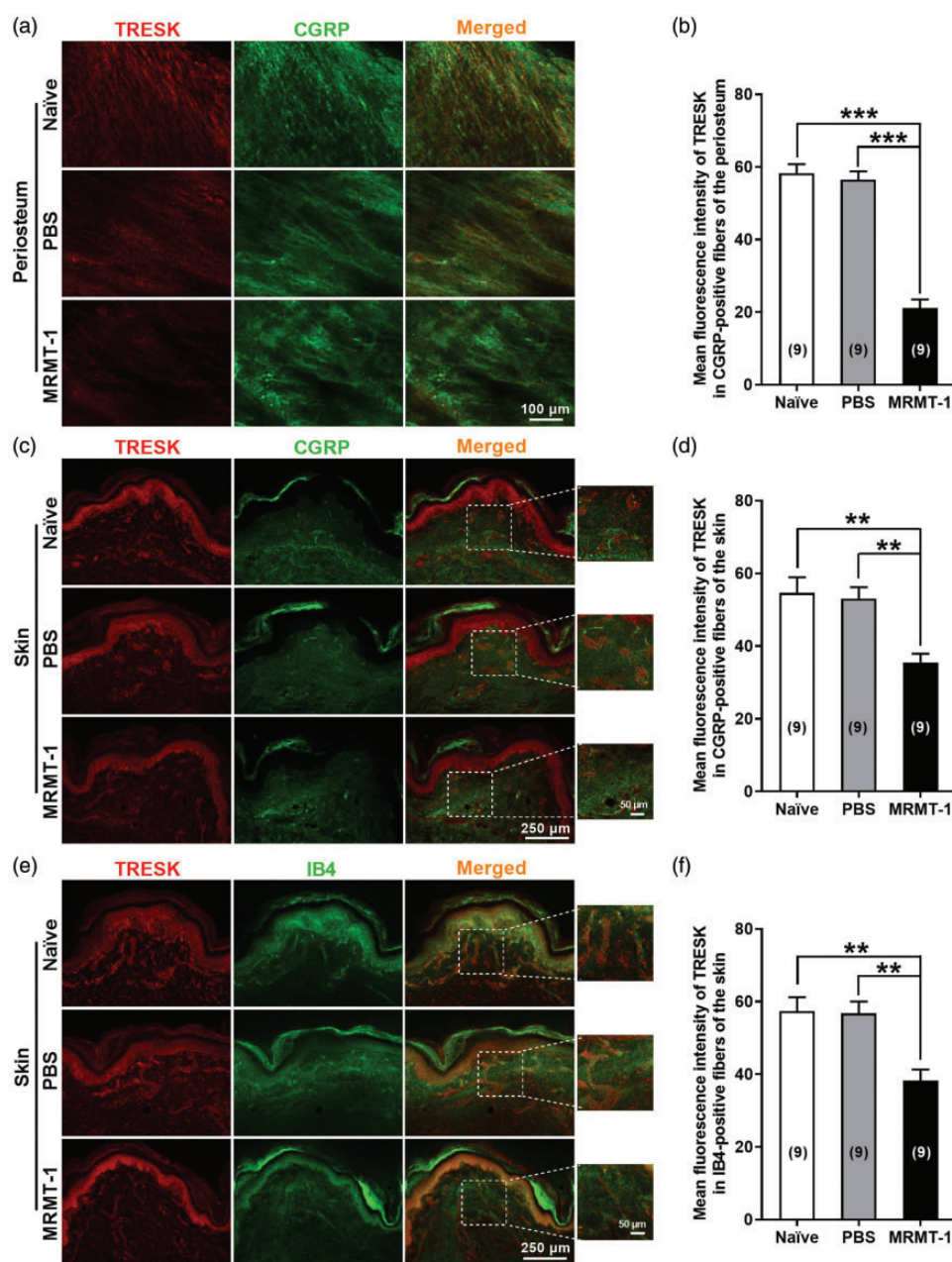


**Figure 3.** Decreased expression of TRESK in the tibial periosteum and the hindpaw skin of bone cancer rats. (a, b) Expression of TRESK in CGRP<sup>+</sup> fibers innervating the tibial periosteum of naïve, PBS- and MRMT-1 (tumor cells)-treated rats. (a) Representative images of immunofluorescence staining with TRESK (red) and CGRP (green) in ipsilateral tibial periosteum on day 14 post-surgery are shown. Scale bar = 100  $\mu\text{m}$ . (b) Statistical analysis for the mean fluorescence intensity of TRESK immunostaining in CGRP<sup>+</sup> fibers of the tibial periosteum. \*\*\*  $p < 0.001$ , one-way ANOVA with Turkey *post-hoc* test,  $n = 9$  visual fields from 3 rats per group. (c, d) Expression of TRESK in CGRP<sup>+</sup> fibers innervating the hindpaw skin of naïve, PBS- and MRMT-1 (tumor cells)-treated rats. (c) Representative images of immunofluorescence staining with TRESK (red) and CGRP (green) in ipsilateral hindpaw skin on day 14 post-surgery are shown. Scale bar = 250  $\mu\text{m}$ . (d) Statistical analysis for the mean fluorescence intensity of TRESK immunostaining in CGRP<sup>+</sup> fibers of the tibial periosteum. \*\*  $p < 0.01$ , one-way ANOVA with Turkey *post-hoc* test,  $n = 9$  visual fields from 3 rats per group. (e, f) Expression of TRESK in IB4<sup>+</sup> fibers innervating the hindpaw skin of naïve, PBS- and MRMT-1 (tumor cells)-treated rats. (e) Representative images of immunofluorescence staining with TRESK (red) and IB4 (green) in ipsilateral hindpaw skin on day 14 post-surgery are shown. Scale bar = 250  $\mu\text{m}$ . (f) Statistical analysis for the mean fluorescence intensity of TRESK immunostaining in IB4<sup>+</sup> fibers of the tibial periosteum. \*\*  $p < 0.01$ , one-way ANOVA with Turkey *post-hoc* test,  $n = 9$  visual fields from 3 rats per group.

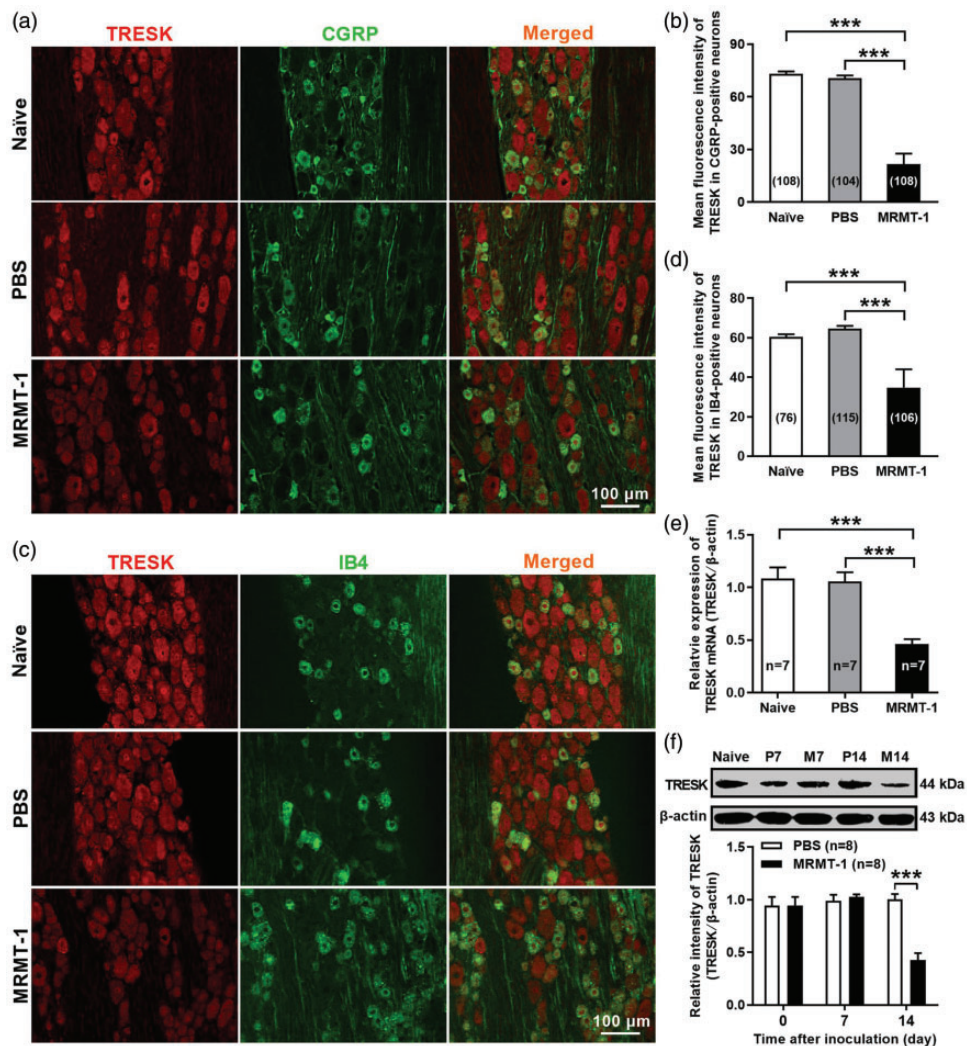


**Figure 4.** Decreased expression of TRESK in the DRG neurons of bone cancer rats. Immunofluorescence staining of TRESK with CGRP (a, b) and IB4 (c, d) in the DRG neurons. (a, b) Expression of TRESK in CGRP<sup>+</sup> DRG neurons of naïve, PBS- and MRMT-1 (tumor cells)-treated rats. (a) Representative images of immunofluorescence staining with TRESK (red) and CGRP (green) in ipsilateral L4/5 DRG neurons on day 14 post-surgery are shown. Scale bar = 100  $\mu$ m. (b) Statistical analysis for the mean fluorescence intensity of TRESK immunostaining in CGRP<sup>+</sup> DRG neurons. \*\*\* $p$  < 0.001, one-way ANOVA with Turkey *post-hoc* test,  $n$  = 104–108 cells from 3 rats per group. (c, d) Expression of TRESK in IB4<sup>+</sup> DRG neurons of naïve, PBS- and MRMT-1 (tumor cells)-treated rats. (a) Representative images of immunofluorescence staining with TRESK (red) and IB4 (green) in ipsilateral L4/5 DRG neurons on day 14 post-surgery are shown. Scale bar = 100  $\mu$ m. (b) Statistical analysis for the mean fluorescence intensity of TRESK immunostaining in IB4<sup>+</sup> DRG neurons. \*\*\* $p$  < 0.001, one-way ANOVA with Turkey *post-hoc* test,  $n$  = 76–115 cells from 3 rats per group. (e) Expression of TRESK mRNA in ipsilateral L4/5 DRGs of naïve, PBS- and MRMT-1 (tumor cells)-treated rats. \*\*\* $p$  < 0.001, one-way ANOVA with Turkey *post-hoc* test,  $n$  = 7 rats per group. (f) Alterations of TRESK protein abundance in ipsilateral L4/5 DRGs before (day 0) and on day 7 and day 14 post-surgery in PBS- and MRMT-1 (tumor cells)-treated rats. \*\*\* $p$  < 0.001, two-way ANOVA with Sidak's *post-hoc* test,  $n$  = 8 rats per group. P, PBS group; M, MRMT-1 group.

0.9  $\pm$  0.3 sec vs. LV-ZsGreen 3.3  $\pm$  0.7 sec,  $p$  = 0.0044,  $F_{3,68}$  = 3.2; SFLn: LV-TRESK 1.6  $\pm$  0.5 events vs. LV-ZsGreen 6.9  $\pm$  1.5 events,  $p$  = 0.0032,  $F_{3,45}$  = 3.13, two-way ANOVA, Figure 5(c) and (d) at the end of our experimental observation. In contrast, the bone cancer-induced cutaneous pain (evoked pain) was alleviated at day 18 but not day 14 after tumor cells inoculation, as indicated by increased paw withdrawal threshold (PWT, LV-TRESK 13.2  $\pm$  0.6g vs. LV-ZsGreen 7.0  $\pm$  1.3g,

$p$  = 0.0008,  $F_{3,42}$  = 2.77, two-way ANOVA, Figure 5(e) rather than paw withdrawal latency (PWL, LV-TRESK 14.3  $\pm$  1.5 sec vs. LV-ZsGreen 11.1  $\pm$  1.3 sec,  $p$  = 0.4022,  $F_{3,42}$  = 0.59, two-way ANOVA, Figure 5(f) on day 18 after tumor cells inoculation in TRESK overexpressed rats. These results suggested that the relief of bone cancer-induced cutaneous pain (evoked pain) is time delayed than spontaneous pain by overexpressing TRESK in DRG neurons.

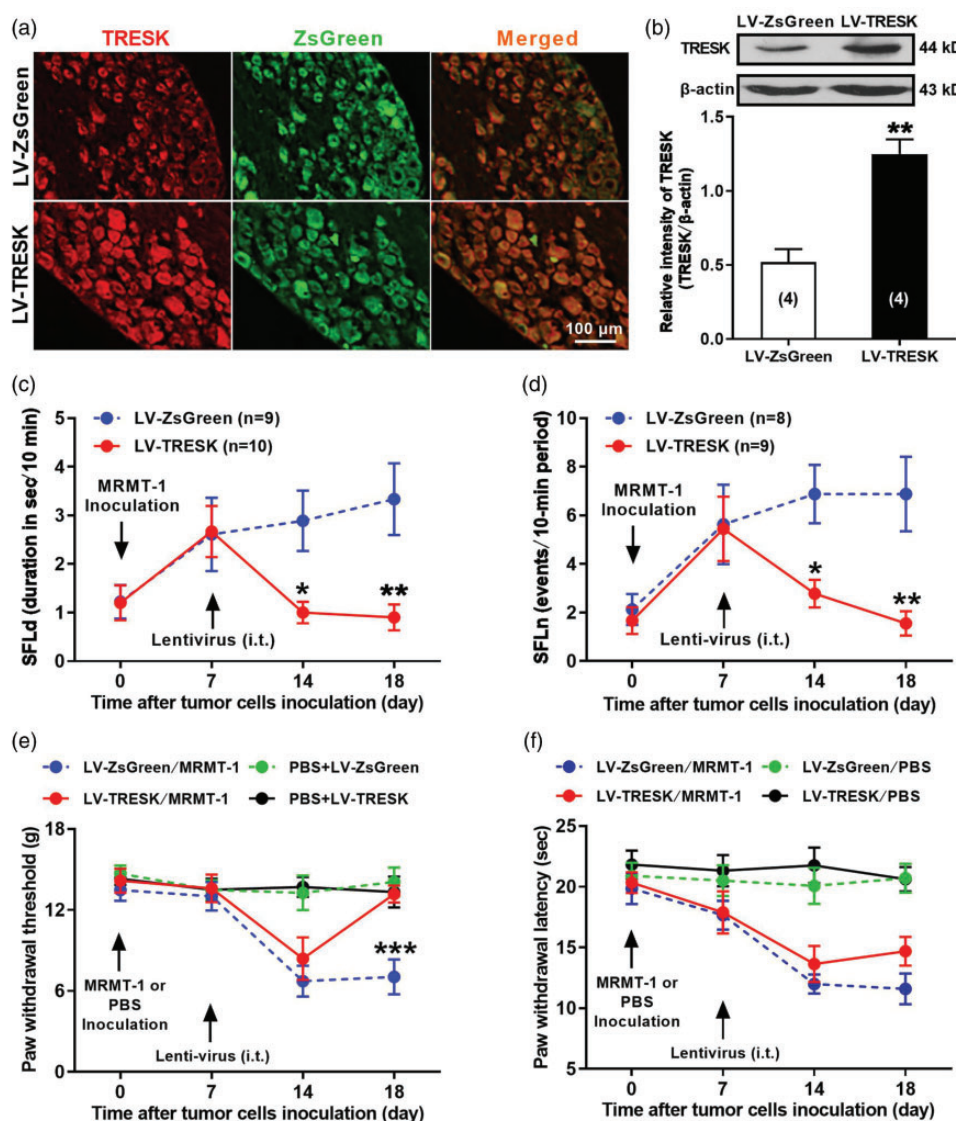


**Figure 5.** Effects of TRESK overexpression on bone cancer-induced spontaneous pain and evoked cutaneous pain in tumor-bearing rats. (a, b) Validation of TRESK overexpression in ipsilateral L4/5 DRG neurons of bone cancer rats received intrathecal injection (i.t.) of lentivirus-expressed TRESK linked ZsGreen (LV-TRESK). (a) Representative images of immunofluorescence staining with TRESK (red) and ZsGreen (green) in DRG neurons are shown. Scale bar = 100  $\mu$ m. (b) TRESK protein abundance in ipsilateral L4/5 DRGs of bone cancer rats received intrathecal LV-TRESK or LV-ZsGreen (control) treatment. \*\* $p < 0.01$ , two-tailed unpaired *t*-test,  $n = 4$  rats per group. (c, d) Effects of i.t. LV-TRESK on bone cancer-induced spontaneous pain in bone cancer rats. Spontaneous foot-lifting (SFL) behaviors including SFL duration (SFLd) (c) and numbers (SFLn) (d) were video recorded to assess the spontaneous pain. \* $p < 0.05$ , \*\* $p < 0.01$ , two-way ANOVA with Sidak's *post-hoc* test,  $n = 8-10$  rats per group. (e, f) Effects of i.t. LV-TRESK on bone cancer-induced cutaneous pain in bone cancer rats. Paw withdrawal threshold (PWT) in response to von Frey filaments stimulation (e) and paw withdrawal latency (PWL) to radiant heat stimulation (f) were measured to assess the evoked cutaneous pain. \*\*\* $p < 0.001$  compared between LV-TRESK/MRMT-1 and the LV-ZsGreen/MRMT-1 groups, two-way ANOVA with Sidak's *post-hoc* test,  $n = 8$  rats per group.

### Knockdown of TRESK in DRG neurons induces spontaneous pain and evoked pain behaviors in naive rats

Furthermore, we investigated whether knockdown of TRESK in DRG neurons by intrathecal delivery of TRESK siRNA could produce spontaneous pain and evoked pain behaviors in naive rats. Knockdown of

TRESK in DRG neurons was validated by a reduction of both TRESK mRNA level (TRESK siRNA  $0.3 \pm 0.1$  vs. Scramble  $1.6 \pm 0.1$ ,  $p < 0.0001$ ,  $t_{10} = 12.25$ , unpaired two-tailed *t*-test, Figure 6(a)) and TRESK protein abundance (TRESK siRNA  $0.5 \pm 0.07$  vs. Scramble  $1.3 \pm 0.04$ ,  $p = 0.0011$ ,  $t_4 = 8.35$ , unpaired two-tailed *t*-test, Figure 6(b)) in the DRG of TRESK siRNA-treated rats. The behavioral results showed that the spontaneous

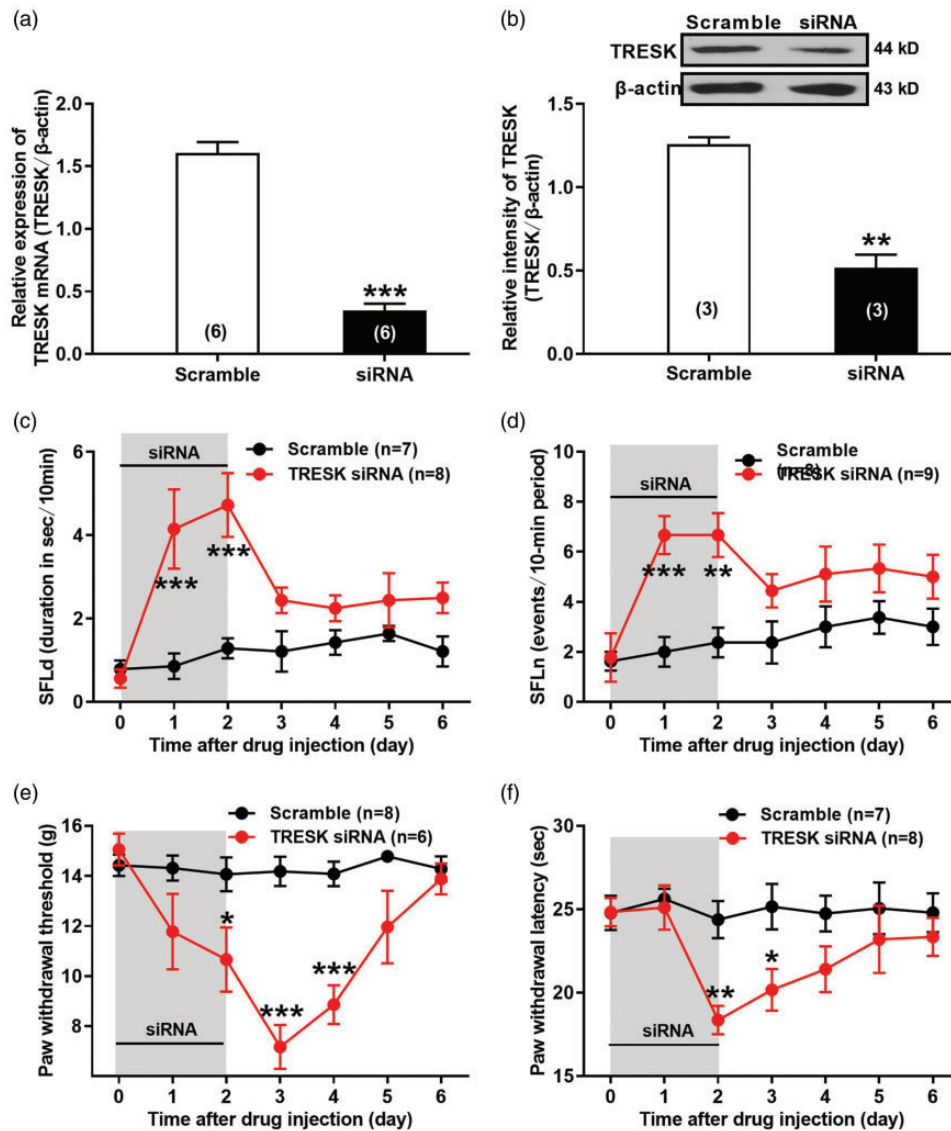


**Figure 6.** Effects of TRESK knockdown on spontaneous pain and evoked pain behaviors in naïve rats. (a, b) Validation of TRESK knockdown in ipsilateral L4/5 DRGs of naïve rats received intrathecal injection (i.t.) of TRESK siRNA. (a) Real-time quantitative PCR (RT-qPCR) assay of TRESK mRNA expression.  $***p < 0.001$ , two-tailed unpaired t-test,  $n = 6$  rats per group. (b) Western blotting assay of TRESK protein abundance.  $***p < 0.001$ , two-tailed unpaired t-test,  $n = 3$  rats per group. (c, d) Effects of i.t. TRESK siRNA on spontaneous pain behaviors of naïve rats. Spontaneous foot-lifting (SFL) behaviors including SFL duration (SFLd) (c) and numbers (SFLn) (d) were video recorded to assess the spontaneous pain.  $**p < 0.01$ ,  $***p < 0.001$ , two-way ANOVA f with Sidak's *post-hoc* test,  $n = 7-9$  rats per group. (e, f) Effects of i.t. TRESK siRNA on evoked cutaneous pain behaviors of naïve rats. Paw withdrawal threshold (PWT) in response to von Frey filaments stimulation (e) and paw withdrawal latency (PWL) to radiant heat stimulation (f) were measured to assess the evoked cutaneous pain.  $*p < 0.05$ ,  $**p < 0.01$ ,  $***p < 0.001$ , two-way ANOVA f with Sidak's *post-hoc* test,  $n = 6-8$  rats per group.

pain, indicated as the spontaneous foot-lifting (SFL) behavior including SFL duration (SFLd) and numbers (SFLn) were both increased on day 1 post-TRESK siRNA administration (SFLd: TRESK siRNA  $4.2 \pm 0.95$  sec vs. Scramble  $0.9 \pm 0.30$  sec,  $p < 0.0001$ ,  $F_{6,91} = 3.98$ ; SFLn: TRESK siRNA  $6.7 \pm 0.8$  events vs. Scramble  $2.0 \pm 0.6$  events,  $p = 0.0007$ ,  $F_{6,105} = 1.81$ ) but disappeared quickly at 3 days after siRNA withdrawal (two-way ANOVA, Figure 6(c) and (d)). In contrast, the

cutaneous pain manifested as evoked pain behaviors including decreased paw withdrawal threshold (PWT) in response to von Frey filaments and paw withdrawal latency (PWL) in response to radiant heat emerged on day 2 post-TRESK siRNA administration (PWT: TRESK siRNA  $10.7 \pm 1.3$ g vs. Scramble  $14.1 \pm 0.7$ g,  $p = 0.0173$ ,  $F_{6,84} = 5.80$ ; PWL: TRESK siRNA  $18.4 \pm 0.9$  sec vs. Scramble  $24.4 \pm 1.1$  sec,  $p = 0.0073$ ,  $F_{6,91} = 1.64$ ) but lasted for a long time (2 days for

PWT and 1 day for PWL) after siRNA withdrawal (two-way ANOVA, Figure 6(e) and (f)). These results revealed that knockdown of TRESK in DRG neurons produce significant spontaneous pain and evoked pain behaviors in naïve rats, suggesting the role of decreased TRESK in the pathogenesis of bone cancer-induced pain.

## Discussion

In this study, we found a wide distribution of TRESK on both CGRP<sup>+</sup> and IB4<sup>+</sup> nerve fibers in the hindpaw skin as well as on CGRP<sup>+</sup> nerve fibers in the tibial periosteum which lacks IB4<sup>+</sup> fibers innervation, and on CGRP<sup>+</sup> and IB4<sup>+</sup> DRG neurons in rats. We also found a significant reduction of TRESK expression in the corresponding nerve fibers within the hindpaw skin, the tibial periosteum and the DRG neurons in bone cancer rats. Overexpression of TRESK in DRG neurons attenuated the bone cancer-induced spontaneous pain and evoked cutaneous pain in tumor-bearing rats. In contrast, knockdown of TRESK in DRG neurons produced both spontaneous pain and evoked pain in naïve rats. Using a battery of skeletal pain-related behaviors (e.g. spontaneous foot lifting, SFL, reduced weight-bearing, sporadic hopping, et al.) and von Frey assessment of mechanical hypersensitivity on the plantar surface of the hind paw (i.e. evoked pain), Guedon et al.<sup>11</sup> have identified the dissociation between the relief of skeletal pain behaviors and skin hypersensitivity in a mouse model of bone cancer pain. The nocifensive behaviors used for assessment of skeletal pain-related behaviors were defined as any of the following: (1) full guarding (lifting the affected limb and holding it against its body), (2) reduced weight-bearing (affected limb is held in such a way that the foot, or the side of the foot, is merely resting on the floor), (3) tending to the affected limb (abnormal grooming behavior directed solely to affected limb, specifically licking lower limb and foot), (4) flinching the affected limb, and (5) sporadic hopping (intermittent jumps without utilizing affected limb). This method is the same as reported in previous studies.<sup>2,50,51</sup> Based on the abovementioned evidence, the spontaneous foot lifting behaviors probably just partly reflects the skeletal pain, while the evoked pain behaviors on the plantar surface of the hind paw mainly reflects the cutaneous pain. Thus, we speculated that the differential distribution and decreased expression of TRESK channels in the periosteum and skin, which is attributed to the lack of IB4<sup>+</sup> fibers innervation within the periosteum of the tibia, probably contribute to the behavioral divergence of bone cancer-induced spontaneous pain (partly reflect skeletal pain) and evoked pain (reflect cutaneous pain) in bone cancer rats.

It is suggested that skeletal pain and cutaneous pain behaviors can be mediated by different types of nerve

fibers in the bone and the skin.<sup>11,12</sup> According to the expression of neuropeptides, receptors, channels and their responses to the growth factors in adulthood, C-fibers (as the main nociceptors) can be divided into two different types including peptide-rich CGRP<sup>+</sup> fibers and peptide-poor IB4<sup>+</sup> fibers.<sup>52,53</sup> CGRP<sup>+</sup> fibers have been shown to express substance P (SP) and tropomyosin receptor kinase A (TrkA), and be regulated by the corresponding ligand, nerve growth factor (NGF).<sup>15</sup> In contrast, IB4<sup>+</sup> fibers have been shown to express the purinergic P2X3 receptor and the GDNF receptor complex, and be regulated by glial cell line-derived neurotrophic factor (GDNF).<sup>16,17</sup> Our results showed that while both CGRP<sup>+</sup> and IB4<sup>+</sup> nerve fibers innervate the skin, only CGRP<sup>+</sup> nerve fibers innervate the periosteum. Consistently, previous studies have demonstrated that P2X3<sup>+</sup>/IB4<sup>+</sup> sensory nerve fibers innervate densely the skin but not the bone, while TrkA<sup>+</sup>/CGRP<sup>+</sup> sensory nerve fibers have the innervation to the bone and skin either.<sup>12,48,49</sup> So the lack of IB4<sup>+</sup> nerve fibers in the bone may explain the limited relief of cancer-induced skeletal pain in mice with anti-P2X3 treatment,<sup>11,18</sup> and may be the potential reason for the divergence of skeletal and cutaneous pain in some circumstance.

The TRESK channel has been regarded as a key component of the resting membrane potential of primary afferent neurons and plays an important role in the regulation of neuronal excitability.<sup>38,54</sup> In this study, we found a wide distribution of TRESK on both CGRP<sup>+</sup> and IB4<sup>+</sup> nerve fibers in the glabrous skin of the hindpaw as well as on the CGRP<sup>+</sup> nerve fibers in the tibial periosteum which lacks IB4<sup>+</sup> fibers innervation, and on both CGRP<sup>+</sup> and IB4<sup>+</sup> DRG neurons in naïve rats. These results are consistent with previous findings showing that the expression of TRESK is found in almost all neurons and especially abundant in small-diameter nociceptive neurons in the DRG.<sup>34</sup> It is reported that TRESK is highly expressed in sensory ganglia<sup>26,29,55-58</sup> within specific subtypes of sensory neurons, mainly nociceptors and especially in non-peptidergic neurons.<sup>30,31,57,59,60</sup> In fact, several RNA sequencing studies in DRG and TG ganglia have provided evidence showing that TRESK is present in a subpopulation of low-threshold mechanoreceptors involved in touch sensation (expressing TRKB and Piezo2) and, predominantly, in non-peptidergic nociceptors.<sup>30-32</sup> Combined RNA *in situ* hybridization (ISH) with immunohistochemistry for molecular markers of canonical sensory neuron populations, Weir et al.<sup>33</sup> have examined the TRESK expression in the TG neurons of mice, and found that TRESK was present in neurons of all soma diameters. Within small diameter neurons that likely represent unmyelinated C-fibers, the TRESK was present in approximately 72% of neurons that bound the IB4<sup>+</sup> neurons, and 29% of CGRP<sup>+</sup> neurons. Whereas

within medium/large diameter neurons, the TRESK was expressed in a large proportion of CGRP<sup>+</sup> neurons (~67%) and neurons highly expressing TRKB<sup>+</sup> (~90%), representing a subset of A $\delta$ -nociceptors and D-hairs respectively. In our present study, we indeed found that the TRESK is expressed in both CGRP<sup>+</sup> (peptidergic) and IB4<sup>+</sup> (non-peptidergic) DRG neurons, however, the number of TRESK/CGRP-positive neurons is lower than that of TRESK/IB4-positive neurons, which is consistent with the results reported by Weir et al.<sup>33</sup> in their previous study.

Moreover, we found that the expression of TRESK protein was decreased in the corresponding nerve fibers within the hindpaw skin, the tibial periosteum and the DRG neurons in tumor-bearing rats, for example, a decreased expression of TRESK was observed on both CGRP<sup>+</sup> and IB4<sup>+</sup> nerve fibers in the hindpaw skin, on CGRP<sup>+</sup> nerve fibers in the tibial periosteum, and on CGRP<sup>+</sup> and IB4<sup>+</sup> DRG neurons in bone cancer rats. In fact, the reduction of TRESK expression and TRESK-mediated background currents are shown in rodent models of inflammatory pain and neuropathic pain.<sup>38,40</sup> Also, Guo et al.<sup>35</sup> found that endogenous TRESK activity regulates trigeminal nociception, and genetic loss of TRESK significantly increases the likelihood of developing headache. Royal et al.<sup>36</sup> demonstrated that migraine-associated frameshift mutations of TRESK lead to the production of a second protein fragment, which carries the pathophysiological function by inhibiting TREK1 and 2, due to a mechanism called frameshift mutation-induced alternative translation initiation (fsATI). Moreover, Castellanos et al.<sup>37</sup> discovered that genetic removal of TRESK specifically enhances mechanical and cold sensitivity in mice, not affecting the sensitivity to other stimuli. Therefore, a decreased expression of TRESK in the periosteum, the skin and the nociceptive DRG neurons likely contributes to the pathogenesis of cancer-induced skeletal pain and cutaneous pain in rats. Indeed, we found an apparent dissociation of bone cancer-induced spontaneous pain (partly reflect skeletal pain) and evoked pain (reflect cutaneous pain) behaviors in tumor-bearing rats. For instance, overexpression of TRESK in DRG neurons attenuated both cancer-induced spontaneous pain and evoked pain in tumor-bearing rats, in which the relief of cutaneous pain (evoked pain) is time delayed than spontaneous pain. In contrast, knockdown of TRESK in DRG neurons produced significant spontaneous pain and evoked pain behaviors in naïve rats, suggesting the role of decreased TRESK in the pathogenesis of bone cancer-induced pain. We speculated that the differential distribution and decreased expression of TRESK in the periosteum and skin, which is attributed to the lack of IB4<sup>+</sup> fibers innervation within the periosteum of the tibia, may be a reason for the dissociation of bone

cancer-induced spontaneous pain and evoked pain in rats. In tumor-bearing rats, the TRESK channels are decreased gradually along with tumor progression in CGRP<sup>+</sup> and IB4<sup>+</sup> small-diameter neurons, in CGRP<sup>+</sup> and IB4<sup>+</sup> nerve fibers innervating the skin, and in CGRP<sup>+</sup> nerve fibers within the periosteum. Thus, intrathecal delivery of lentivirus-expressed TRESK (LV-TRESK) could rescue the decreased TRESK channels within the periosteum, the skin, and the nociceptive DRG neurons, subsequently attenuating the cancer-induced spontaneous pain and evoked pain in bone cancer rats. It is because only one type of CGRP<sup>+</sup> nerve fibers innervate the periosteum, whereas both CGRP<sup>+</sup> and IB4<sup>+</sup> nerve fibers are existed in skin, so the decreased TRESK abundance within the bone is much easy to be restored than that within the skin in tumor-bearing rats received LV-TRESK treatment. As a result, the cancer-induced spontaneous pain (partly reflect skeletal pain) is easy to be alleviated than the evoked cutaneous pain after TRESK overexpression.

On the other hand, because the lacks of IB4<sup>+</sup> nerve fibers innervation within the periosteum whereas there have both CGRP<sup>+</sup> and IB4<sup>+</sup> nerve fibers innervation within the skin, so intrathecal delivery of TRESK siRNA is easy to knock down TRESK in the periosteum than that in the skin. Hence, a slight reduction of TRESK in CGRP<sup>+</sup> fiber innervating the periosteum is enough to induce spontaneous pain, whereas only when a wide distributed TRESK was knocked down in both CGRP<sup>+</sup> and IB4<sup>+</sup> fibers innervating the skin can lead to the evoked cutaneous pain in naïve rats with intrathecal TRESK siRNA application. These may be a possible reason for explaining our present findings to show that knockdown of TRESK in DRG neurons induced a rapid and transient skeletal pain but a delayed and prolonged cutaneous pain in naïve rats.

In addition, because there is no direct damage to the skin in the model of bone cancer pain, we speculated that the hypersensitivity of nearby skin is also probably derived from cancer-induced skeletal pain, which may be considered as an alternative explanation for the delayed response of cutaneous pain behaviors under both TRESK overexpression and knockdown conditions. Sensitization in different site of pain pathway likely underlies the skeletal pain-induced skin hypersensitivity. The injury-induced infiltration of macrophages and pathological sprouting in DRG lead to the hyperexcitability of the sensory neurons innervating the undamaged skin,<sup>61-63</sup> while central sensitization in the spinal cord and brain can also be the potential mechanism underlying this phenomenon.<sup>64-66</sup>

Of course, our present study has several potential limitations. First, although a prominent effect of TRESK overexpression or knockdown has been shown in DRG neurons, we still cannot rule out the role for the

spinal cord in cancer-induced skeletal pain and cutaneous pain owing to the intrathecal delivery of LV-TRESK or siRNA in our experiments. The difference between skeletal pain and cutaneous pain is probably partially due to the role of central sensitization. In the spinal cord, downregulated TRESK in dorsal horn neurons mediates inflammation and apoptosis via activation of the MAPK pathway in SNI rats.<sup>67</sup> To exclude the influence of spinal cord TRESK, local intra-DRG injection or spinal nerve injection<sup>68,69</sup> for the delivery of LV-TRESK or TRESK siRNA is a preferable choice in this case. Second, owing to the extensive expression of TRESK on nociceptive sensory neurons, the intervening methods for the TRESK cannot be restricted to a particular type of fibers just like anti-NGF or anti-P2X3.<sup>11</sup> To get a better understanding for the contribution of TRESK in cancer-induced skeletal pain and cutaneous pain, we should use specific promoters to induce TRESK overexpression or knockdown targeting CGRP<sup>+</sup> and IB4<sup>+</sup> fibers respectively and elucidate the mechanisms underlying the behavioral divergence of cancer-induced skeletal pain and cutaneous pain. Third, there is a doubt whether spontaneous pain behaviors reflect skeletal pain faithfully without the mix of cutaneous pain. It has been shown that severe injury to the skin induces remarkable changes in mechanical sensitivity of the foot and therefore affect the ability to place weight on the damaged foot.<sup>70</sup> A feasible way is to measure the skeletal pain with local anesthetics on hindpaw, which is inspired by a clinic trial.<sup>10</sup> Nevertheless, considering the dissociation of skeletal pain and skin hypersensitivity in our animal model, the interruption can be ignored.

In conclusion, our present data suggested the differential distribution and decreased expression of TRESK channels in the periosteum and skin, which is attributed to the lack of IB4<sup>+</sup> fibers innervation within the periosteum of the tibia, probably contribute to the behavioral divergence of cancer-induced (partly reflect skeletal pain) and evoked pain (reflect cutaneous pain) in bone cancer rats.

### Acknowledgments

We thank X. Gasull (University of Barcelona, Barcelona, Spain) for providing the rat TRESK plasmid.

### Author Contributions

GGX conceived the project, designed the experiments and revised the manuscript. JPL and HBJ performed most of experiments, acquired and analyzed data, and drafted the manuscript. KX, ZXZ, ZRJ, SQC, and YT performed some of experiments and help data analysis. JC provided expertise and technique guidance. All authors have read and approved the final manuscript.

### Declaration of Conflicting Interests

The author(s) declared no potential conflicts of interest with respect to the research, authorship, and/or publication of this article.

### Funding

The author(s) disclosed receipt of the following financial support for the research, authorship, and/or publication of this article: This research was funded by the grants from National Natural Science Foundation of China (81974169, 81671085, 61527815), National Key R&D Program of China (2019YFC1712104), and the National Defense Science and Technology Innovation Special Zone Project (19-H863-04-LZ-001-006-04).

### ORCID iD

Guo-Gang Xing  <https://orcid.org/0000-0001-5670-4857>

### Supplemental Material

Supplemental material for this article is available online.

### References

- Migliorini F, Maffulli N, Trivellas A, Eschweiler J, Tingart M, Driessen A. Bone metastases: a comprehensive review of the literature. *Mol Biol Rep* 2020; 47: 6337–6345.
- McCaffrey G, Thompson ML, Majuta L, Fealk MN, Chartier S, Longo G, Mantyh PW. NGF blockade at early times during bone cancer development attenuates bone destruction and increases limb use. *Cancer Res* 2014; 74: 7014–7023.
- Majuta LA, Guedon JG, Mitchell SAT, Kuskowski MA, Mantyh PW. Mice with cancer-induced bone pain show a marked decline in day/night activity. *Pain Rep* 2017; 2: e614.
- Scott AC, McConnell S, Laird B, Colvin L, Fallon M. Quantitative Sensory Testing to assess the sensory characteristics of cancer-induced bone pain after radiotherapy and potential clinical biomarkers of response. *Eur J Pain* 2012; 16: 123–133.
- Zheng Q, Fang D, Liu M, Cai J, Wan Y, Han JS, Xing GG. Suppression of KCNQ/M (Kv7) potassium channels in dorsal root ganglion neurons contributes to the development of bone cancer pain in a rat model. *Pain* 2013; 154: 434–448.
- Yang Y, Li S, Jin ZR, Jing HB, Zhao HY, Liu BH, Liang YJ, Liu LY, Cai J, Wan Y, Xing GG. Decreased abundance of TRESK two-pore domain potassium channels in sensory neurons underlies the pain associated with bone metastasis. *Sci Signal* 2018; 11: eaao5150.
- Zhu YF, Ungard R, Zagal N, Huizinga JD, Henry JL, Singh G. Rat model of cancer-induced bone pain: changes in nonnociceptive sensory neurons in vivo. *Pain Rep* 2017; 2: e603.
- Zhou YL, Jiang GQ, Wei J, Zhang HH, Chen W, Zhu H, Hu S, Jiang X, Xu GY. Enhanced binding capability of nuclear factor-kappaB with demethylated P2X3 receptor

- gene contributes to cancer pain in rats. *Pain* 2015; 156: 1892–1905.
9. Hald A, Nedergaard S, Hansen RR, Ding M, Heegaard AM. Differential activation of spinal cord glial cells in murine models of neuropathic and cancer pain. *Eur J Pain* 2009; 13: 138–145.
  10. Andresen T, Pfeiffer-Jensen M, Brock C, Drewes AM, Arendt-Nielsen L. A human experimental bone pain model. *Basic Clin Pharmacol Toxicol* 2013; 112: 116–123.
  11. Guedon JM, Longo G, Majuta LA, Thomsson ML, Fealk MN, Mantyh PW. Dissociation between the relief of skeletal pain behaviors and skin hypersensitivity in a model of bone cancer pain. *Pain* 2016; 157: 1239–1247.
  12. Jimenez-Andrade JM, Mantyh WG, Bloom AP, Xu H, Ferng AS, Dussor G, Vanderah TW, Mantyh PW. A phenotypically restricted set of primary afferent nerve fibers innervate the bone versus skin: therapeutic opportunity for treating skeletal pain. *Bone* 2010; 46: 306–313.
  13. Mantyh P. Bone cancer pain: causes, consequences, and therapeutic opportunities. *Pain* 2013; 154: S54–S62.
  14. Mach DB, Rogers SD, Sabino MC, Luger NM, Schwei MJ, Pomonis JD, Keyser CP, Clohisey DR, Adams DJ, O'Leary P, Mantyh PW. Origins of skeletal pain: sensory and sympathetic innervation of the mouse femur. *Neuroscience* 2002; 113: 155–166.
  15. Averill S, McMahon SB, Clary DO, Reichardt LF, Priestley JV. Immunocytochemical localization of trkA receptors in chemically identified subgroups of adult rat sensory neurons. *Eur J Neurosci* 1995; 7: 1484–1494.
  16. Molliver DC, Wright DE, Leitner ML, Parsadanian AS, Doster K, Wen D, Yan Q, Snider WD. IB4-binding DRG neurons switch from NGF to GDNF dependence in early postnatal life. *Neuron* 1997; 19: 849–861.
  17. Bradbury EJ, Burnstock G, McMahon SB. The expression of P2X3 purinoreceptors in sensory neurons: effects of axotomy and glial-derived neurotrophic factor. *Mol Cell Neurosci* 1998; 12: 256–268.
  18. Hansen RR, Nasser A, Falk S, Baldvinsson SB, Ohlsson PH, Bahl JM, Jarvis MF, Ding M, Heegaard AM. Chronic administration of the selective P2X3, P2X2/3 receptor antagonist, A-317491, transiently attenuates cancer-induced bone pain in mice. *Eur J Pharmacol* 2012; 688: 27–34.
  19. Koewler NJ, Freeman KT, Buus RJ, Herrera MB, Jimenez-Andrade JM, Ghilardi JR, Peters CM, Sullivan LJ, Kuskowski MA, Lewis JL, Mantyh PW. Effects of a monoclonal antibody raised against nerve growth factor on skeletal pain and bone healing after fracture of the C57BL/6J mouse femur. *J Bone Miner Res* 2007; 22: 1732–1742.
  20. Zhao J, Pan HL, Li TT, Zhang YQ, Wei JY, Zhao ZQ. The sensitization of peripheral C-fibers to lysophosphatidic acid in bone cancer pain. *Life Sci* 2010; 87: 120–125.
  21. Zheng Q, Fang D, Cai J, Wan Y, Han JS, Xing GG. Enhanced excitability of small dorsal root ganglion neurons in rats with bone cancer pain. *Mol Pain* 2012; 8: 24.
  22. Hua B, Gao Y, Kong X, Yang L, Hou W, Bao Y. New insights of nociceptor sensitization in bone cancer pain. *Expert Opin Ther Targets* 2015; 19: 227–243.
  23. Liu XD, Yang JJ, Fang D, Cai J, Wan Y, Xing GG. Functional upregulation of nav1.8 sodium channels on the membrane of dorsal root Ganglia neurons contributes to the development of cancer-induced bone pain. *PLoS One* 2014; 9: e114623.
  24. Fang D, Kong LY, Cai J, Li S, Liu XD, Han JS, Xing GG. Interleukin-6-mediated functional upregulation of TRPV1 receptors in dorsal root ganglion neurons through the activation of JAK/PI3K signaling pathway: roles in the development of bone cancer pain in a rat model. *Pain* 2015; 156: 1124–1144.
  25. Enyedi P, Czirjak G. Properties, regulation, pharmacology, and functions of the K(2)p channel, TRESK. *Pflugers Arch* 2015; 467: 945–958.
  26. Dobler T, Springauf A, Tovornik S, Weber M, Schmitt A, Sedlmeier R, Wischmeyer E, Doring F. TRESK two-pore-domain K<sup>+</sup> channels constitute a significant component of background potassium currents in murine dorsal root ganglion neurones. *J Physiol* 2007; 585: 867–879.
  27. Tulleuda A, Cokic B, Callejo G, Saiani B, Serra J, Gasull X. TRESK channel contribution to nociceptive sensory neurons excitability: modulation by nerve injury. *Mol Pain* 2011; 7: 30.
  28. Li XY, Toyoda H. Role of leak potassium channels in pain signaling. *Brain Res Bull* 2015; 119: 73–79.
  29. Lafrenière RG, Cader MZ, Poulin JF, Andres-Enguix I, Simoneau M, Gupta N, Boisvert K, Lafrenière F, McLaughlan S, Dubé MP, Marcinkiewicz MM, Ramagopalan S, Ansoorge O, Brais B, Sequeiros J, Pereira-Monteiro JM, Griffiths LR, Tucker SJ, Ebers G, Rouleau GA. A dominant-negative mutation in the TRESK potassium channel is linked to familial migraine with aura. *Nat Med* 2010; 16: 1157–1160.
  30. Usoskin D, Furlan A, Islam S, Abdo H, Lönnerberg P, Lou D, Hjerling-Leffler J, Haeggström J, Kharchenko O, Kharchenko PV, Linnarsson S, Ernfors P. Unbiased classification of sensory neuron types by large-scale single-cell RNA sequencing. *Nat Neurosci* 2015; 18: 145–153.
  31. Zheng Y, Liu P, Bai L, Trimmer JS, Bean BP, Ginty DD. Deep sequencing of somatosensory neurons reveals molecular determinants of intrinsic physiological properties. *Neuron* 2019; 103: 598.e597–616.e597.
  32. Zeisel A, Hochgerner H, Lönnerberg P, Johnsson A, Memic F, van der Zwan J, Häring M, Braun E, Borm LE, La Manno G, Codeluppi S, Furlan A, Lee K, Skene N, Harris KD, Hjerling-Leffler J, Arenas E, Ernfors P, Marklund U, Linnarsson S. Molecular architecture of the mouse nervous system. *Cell* 2018; 174: 999. e1022–1014.e1022.
  33. Weir GA, Pettingill P, Wu Y, Duggal G, Ilie AS, Akerman CJ, Cader MZ. The role of TRESK in discrete sensory neuron populations and somatosensory processing. *Front Mol Neurosci* 2019; 12: 170.
  34. Yoo S, Liu J, Sabbadini M, Au P, Xie GX, Yost CS. Regional expression of the anesthetic-activated potassium channel TRESK in the rat nervous system. *Neurosci Lett* 2009; 465: 79–84.



35. Guo Z, Qiu CS, Jiang X, Zhang J, Li F, Liu Q, Dhaka A, Cao YQ. TRESK K(+) channel activity regulates trigeminal nociception and headache. *eNeuro* 2019; 6: ENEURO.0236-19.2019.
36. Royal P, Andres-Bilbe A, Ávalos Prado P, Verkest C, Wdziekonski B, Schaub S, Baron A, Lesage F, Gasull X, Levitz J, Sandoz G. Migraine-associated TRESK mutations increase neuronal excitability through alternative translation initiation and inhibition of TREK. *Neuron* 2019; 101: 232.e236–245.e236.
37. Castellanos A, Pujol-Coma A, Andres-Bilbe A, Negm A, Callejo G, Soto D, Noël J, Comes N, Gasull X. TRESK background K(+) channel deletion selectively uncovers enhanced mechanical and cold sensitivity. *J Physiol* 2020; 598: 1017–1038.
38. Marsh B, Acosta C, Djouhri L, Lawson SN. Leak K(+) channel mRNAs in dorsal root ganglia: relation to inflammation and spontaneous pain behaviour. *Mol Cell Neurosci* 2012; 49: 375–386.
39. Kollert S, Dombert B, Doring F, Wischmeyer E. Activation of TRESK channels by the inflammatory mediator lysophosphatidic acid balances nociceptive signalling. *Sci Rep* 2015; 5: 12548.
40. Zhou J, Yang CX, Zhong JY, Wang HB. Intrathecal TRESK gene recombinant adenovirus attenuates spared nerve injury-induced neuropathic pain in rats. *Neuroreport* 2013; 24: 131–136.
41. Zimmermann M. Ethical guidelines for investigations of experimental pain in conscious animals. *Pain* 1983; 16: 109–110.
42. Cai J, Fang D, Liu XD, Li S, Ren J, Xing GG. Suppression of KCNQ/M (Kv7) potassium channels in the spinal cord contributes to the sensitization of dorsal horn WDR neurons and pain hypersensitivity in a rat model of bone cancer pain. *Oncol Rep* 2015; 33: 1540–1550.
43. Acosta C, Djouhri L, Watkins R, Berry C, Bromage K, Lawson SN. TREK2 expressed selectively in IB4-binding C-fiber nociceptors hyperpolarizes their membrane potentials and limits spontaneous pain. *J Neurosci* 2014; 34: 1494–1509.
44. Liu M, Yang H, Fang D, Yang JJ, Cai J, Wan Y, Chui DH, Han JS, Xing GG. Upregulation of P2X3 receptors by neuronal calcium sensor protein VILIP-1 in dorsal root ganglions contributes to the bone cancer pain in rats. *Pain* 2013; 154: 1551–1568.
45. Chaplan SR, Bach FW, Pogrel JW, Chung JM, Yaksh TL. Quantitative assessment of tactile allodynia in the rat paw. *J Neurosci Methods* 1994; 53: 55–63.
46. Dixon WJ. Efficient analysis of experimental observations. *Annu Rev Pharmacol Toxicol* 1980; 20: 441–462.
47. Zimmermann M. Pathobiology of neuropathic pain. *Eur J Pharmacol* 2001; 429: 23–37.
48. Martin CD, Jimenez-Andrade JM, Ghilardi JR, Mantyh PW. Organization of a unique net-like meshwork of CGRP+ sensory fibers in the mouse periosteum: implications for the generation and maintenance of bone fracture pain. *Neurosci Lett* 2007; 427: 148–152.
49. Lu J, Zhou XF, Rush RA. Small primary sensory neurons innervating epidermis and viscera display differential phenotype in the adult rat. *Neurosci Res* 2001; 41: 355–363.
50. Halvorson KG, Kubota K, Sevcik MA, Lindsay TH, Sotillo JE, Ghilardi JR, Rosol TJ, Boustany L, Shelton DL, Mantyh PW. A blocking antibody to nerve growth factor attenuates skeletal pain induced by prostate tumor cells growing in bone. *Cancer Res* 2005; 65: 9426–9435.
51. Jimenez-Andrade JM, Martin CD, Koewler NJ, Freeman KT, Sullivan LJ, Halvorson KG, Barthold CM, Peters CM, Buus RJ, Ghilardi JR, Lewis JL, Kuskowski MA, Mantyh PW. Nerve growth factor sequestering therapy attenuates non-malignant skeletal pain following fracture. *Pain* 2007; 133: 183–196.
52. Hunt SP, Mantyh PW. The molecular dynamics of pain control. *Nat Rev Neurosci* 2001; 2: 83–91.
53. Priestley JV, Michael GJ, Averill S, Liu M, Willmott N. Regulation of nociceptive neurons by nerve growth factor and glial cell line derived neurotrophic factor. *Can J Physiol Pharmacol* 2002; 80: 495–505.
54. Zhou J, Chen H, Yang C, Zhong J, He W, Xiong Q. Reversal of TRESK downregulation alleviates neuropathic pain by inhibiting activation of gliocytes in the spinal cord. *Neurochem Res* 2017; 42: 1288–1298.
55. Ray P, Torck A, Quigley L, Wangzhou A, Neiman M, Rao C, Lam T, Kim JY, Kim TH, Zhang MQ, Dussor G, Price TJ. Comparative transcriptome profiling of the human and mouse dorsal root ganglia: an RNA-seq-based resource for pain and sensory neuroscience research. *Pain* 2018; 159: 1325–1345.
56. LaPaglia DM, Sapio MR, Burbelo PD, Thierry-Mieg J, Thierry-Mieg D, Raithel SJ, Ramsden CE, Iadarola MJ, Mannes AJ. RNA-Seq investigations of human post-mortem trigeminal ganglia. *Cephalalgia* 2018; 38: 912–932.
57. Nguyen MQ, Wu Y, Bonilla LS, von Buchholtz LJ, Ryba NJP. Diversity amongst trigeminal neurons revealed by high throughput single cell sequencing. *PLoS One* 2017; 12: e0185543.
58. Kang D, Kim D. TREK-2 (K2P10.1) and TRESK (K2P18.1) are major background K+ channels in dorsal root ganglion neurons. *Am J Physiol Cell Physiol* 2006; 291: C138–C146.
59. Chiu IM, Barrett LB, Williams EK, Strohlic DE, Lee S, Weyer AD, Lou S, Bryman GS, Roberson DP, Ghasemlou N, Piccoli C, Ahat E, Wang V, Cobos EJ, Stucky CL, Ma Q, Liberles SD, Woolf CJ. Transcriptional profiling at whole population and single cell levels reveals somatosensory neuron molecular diversity. *Elife* 2014; 3: e04660.
60. Li CL, Li KC, Wu D, Chen Y, Luo H, Zhao JR, Wang SS, Sun MM, Lu YJ, Zhong YQ, Hu XY, Hou R, Zhou BB, Bao L, Xiao HS, Zhang X. Somatosensory neuron types identified by high-coverage single-cell RNA-sequencing and functional heterogeneity. *Cell Res* 2016; 26: 83–102.
61. Peters CM, Ghilardi JR, Keyser CP, Kubota K, Lindsay TH, Luger NM, Mach DB, Schwei MJ, Sevcik MA, Mantyh PW. Tumor-induced injury of primary afferent sensory nerve fibers in bone cancer pain. *Exp Neurol* 2005; 193: 85–100.
62. Nakajima T, Ohtori S, Yamamoto S, Takahashi K, Harada Y. Differences in innervation and innervated neurons between hip and inguinal skin. *Clin Orthop Relat Res* 2008; 466: 2527–2532.

63. Jimenez-Andrade JM, Bloom AP, Stake JI, Mantyh WG, Taylor RN, Freeman KT, Ghilardi JR, Kuskowski MA, Mantyh PW. Pathological sprouting of adult nociceptors in chronic prostate cancer-induced bone pain. *J Neurosci* 2010; 30: 14649–14656.
64. Mantyh PW. Bone cancer pain: from mechanism to therapy. *Curr Opin Support Palliat Care* 2014; 8: 83–90.
65. Yanagisawa Y, Furue H, Kawamata T, Uta D, Yamamoto J, Furuse S, Katafuchi T, Imoto K, Iwamoto Y, Yoshimura M. Bone cancer induces a unique central sensitization through synaptic changes in a wide area of the spinal cord. *Mol Pain* 2010; 6: 38.
66. Urch CE, Donovan-Rodriguez T, Dickenson AH. Alterations in dorsal horn neurones in a rat model of cancer-induced bone pain. *Pain* 2003; 106: 347–356.
67. Zhou J, Lin W, Chen H, Fan Y, Yang C. TRESK contributes to pain threshold changes by mediating apoptosis via MAPK pathway in the spinal cord. *Neuroscience* 2016; 339: 622–633.
68. Fischer G, Kostic S, Nakai H, Park F, Sapunar D, Yu H, Hogan Q. Direct injection into the dorsal root ganglion: technical, behavioral, and histological observations. *J Neurosci Methods* 2011; 199: 43–55.
69. Chang MF, Hsieh JH, Chiang H, Kan HW, Huang CM, Chellis L, Lin BS, Miaw SC, Pan CL, Chao CC, Hsieh ST. Effective gene expression in the rat dorsal root ganglia with a non-viral vector delivered via spinal nerve injection. *Sci Rep* 2016; 6:35612.
70. Tetreault P, Dansereau MA, Dore-Savard L, Beaudet N, Sarret P. Weight bearing evaluation in inflammatory, neuropathic and cancer chronic pain in freely moving rats. *Physiol Behav* 2011; 104: 495–502.